Int. Journ. of Laser Science, Vol. 1, pp. 31–52
Reprints available directly from the publisher.
Photocopying permitted by license only.

Design and Construction of a Two Degrees of Freedom Laser Linear Encoder in a Littrow Configuration

J-Z. CUI, M. ZHANG*, Y. ZHU, C. NI AND S-Q. DING

Department of Mechanical Engineering, Tsinghua University, Beijing 100084, China

We propose herein a new optical sensor head designed in Littrow configuration for laser linear encoder which can directly measure *X*-direction and *Z*-direction displacement of a linear stage using one-dimensional (1-D) gratings. Given the benefits of Littrow configuration, the measuring range along *Z*-direction is extremely enlarged compared with traditional encoders. Finally, the optical configuration was successfully constructed and its measurement performance was evaluated and analysed. Under non-environmentally controlled conditions, the maximum positioning error in a movement of 2.0 mm was 0.261 µm with a standard deviation of 0.134 µm in the *X*-direction and 0.211 µm with a standard deviation of 0.070 µm in the *Z*-direction.

Keywords: Laser linear encoder, grating interferometer, Littrow configuration, two degrees of freedom, displacement measurement, Doppler effect

1 INTRODUCTION

Laser linear encoder, using a scale grating to generate interference signals proportional to grating displacement, is capable of measuring micro displacement and can be less sensitive to environment disturbances compared with traditional laser interferometer [1]. Linear encoder based on principle of Morié fringes has already been adopted in industry for long-stroke measurement, but its resolution and accuracy is limited due to its large grating pitch [2]. In recent years, laser linear encoder's resolution has achieved nano scale [3–5]. When it comes to two-dimensional (2-D) positioning, however,

*Corresponding author: Tel: +86 (0)10 6279 7393; E-mail: zm01@mails.tsinghua.edu.cn

traditional sensors using a pair of one-dimensional (1-D) sensors in a cross configuration are quite inconvenient and the alignment tolerance is critical and subjected to metrology errors [6]. In a word, it is quite important to develop a 2-D displacement sensor with high resolution and high accuracy.

Among the grating based on two degrees of freedom laser linear encoders developed so far, their scale grating is whether 1-D or 2-D gratings. Most of the linear encoders using 1-D gratings are able to measure displacement along the grating vector direction (*X*-direction in Figure 1) and the grating normal direction (*Z*-direction in Figure 1) [7–11]. Still, the measuring range along the grating normal direction is limited, as the grating motion may change the path of the laser, making the encoders unable to work. While the encoders using 2-D gratings do not display such problems [12–16]. Their measuring range only depends on the size of the gratings; however, when measuring a large-scale in-plane motion, as shown in Figure 1(a), 2-D scale gratings have to be made as large as the measuring area, making the scale gratings quite heavy and not convenient as well. What is more, 2-D gratings are also much more expensive than 1-D gratings as the manufacturing difficulty on large size 2-D gratings is much greater than that on 1-D strip gratings.

Among the linear encoders described above, those designed in a Littrow configuration are able to work normally in a variety of translational motion cases, making them well suited for measuring multi-degree-of-freedom translation. On this basis we proposed a new laser linear encoder designed in Littrow configuration which can directly measure two degrees of freedom using 1-D gratings. Given the benefits from Littrow configuration, the measuring range along the grating normal direction has substantially enlarged.

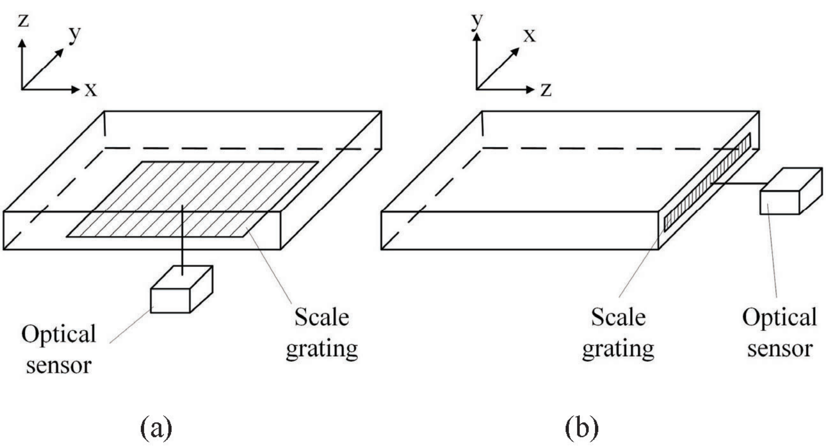

FIGURE 1
Schematic diagram showing measurement of large-stroke plane motion for (a) the 2-D grating sensor and (b) the 1-D grating sensor.

By putting the scale grating on the side of the measuring target, as shown in Figure 1(b), we can achieve the same measuring function and the size of the gratings does not have to be too large. We describe the configuration as well as its measuring performance based on our experimental data and results.

2 OPTICAL CONFIGURATION

The two degrees of freedom laser linear encoder, is consist of four different subsystems: optical sensor head; 1-D scale grating; and two groups of circular polarization configurations, as shown in Figure 2.

Figure 3 shows the optical structure of the sensor head. The optical sensor head is composed of a polarization beam splitter (PBS), a beam splitter (BS), two quarter-wave plate (QW) and several mirrors placed at specific positions. All these optical elements are surrounded by a centre PBS. We create an *X,Y,Z* coordinate system whose *z*-axis is always aligned along the laser beam direction. The *x*-axis is horizontal, aligned along the transmitted polarization direction of the PBS and the *y*-axis is vertical, aligned along the reflected polarization direction of the PBS, as shown in Figure 3. The laser source emits a linearly polarized laser beam whose polarization direction is adjusted to be 45° in the *XOY* plane of the coordinate system. At first, the laser beam is split into a reflected laser beam (R) and a transmitted laser beam (T) after passing a BS and R beam reflected by Mirror 1 turns into the parallel direction with transmitted laser beam (T). These two laser beams both pass through the centre PBS and are divided into two beams respectively. The R beam divides into reflected laser beam (R-R) and transmitted laser beam (R-T)

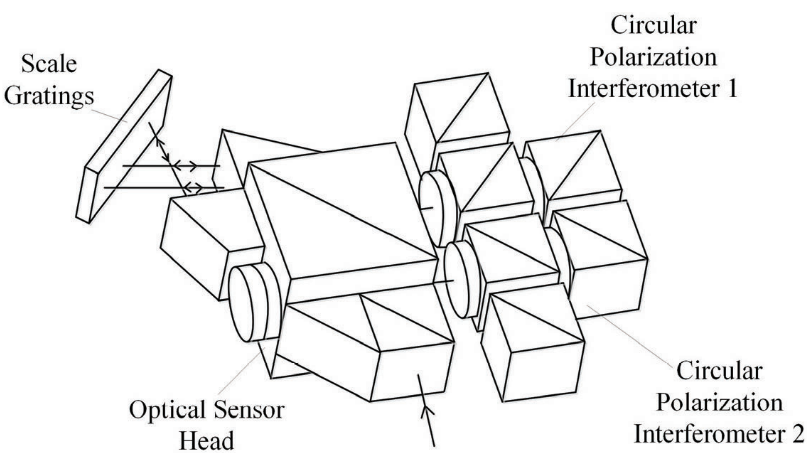

FIGURE 2
Schematic diagram of the optical configuration.

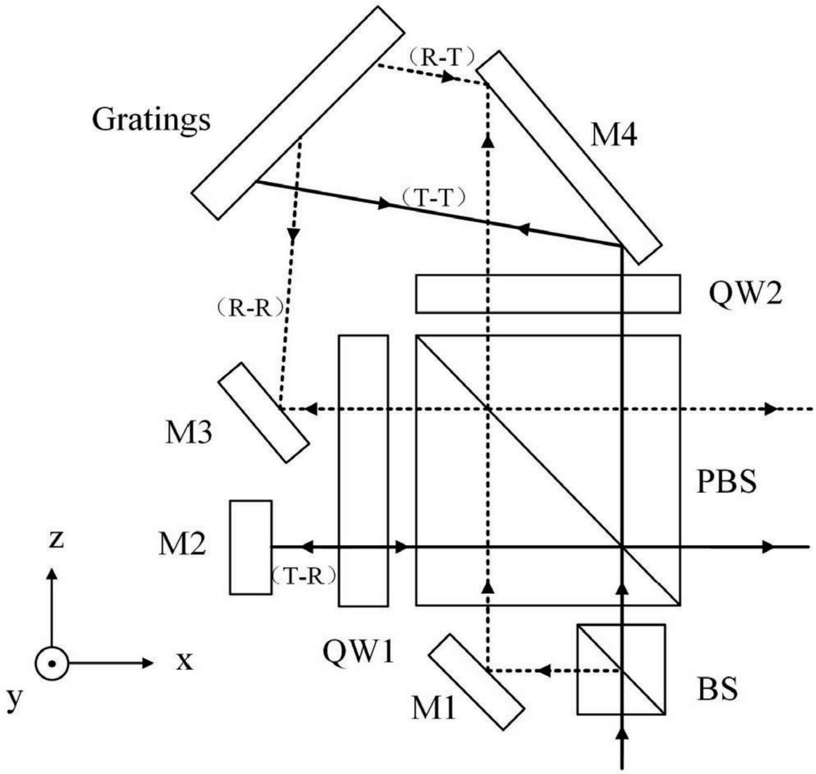

FIGURE 3
Schematic diagram of the optical sensor head.

while the T beam divides into reflected laser beam (T-R) and transmitted laser beam (T-T).

The two reflected beams, R-R and T-R, are both S-polarized. They pass through QW1 whose fast axis is set at 45 ° in the coordinate system and turned into circularly polarized laser. Then they are, respectively, reflected by Mirror 2 and Mirror 3. Mirror 2 is set vertical respected to the direction of the T-R beam, so that the T-R beam is reflected back in the incident direction, passing through QW1 again and then the centre PBS and incidents into Circular Polarization Configuration 2. As the direction of the beam changes after reflection, the angle of the QW1's fast axis has changed into 135.0° in the coordinate system as shown in Figure 4. R-R beam is reflected by Mirror 3 and turns into a direction where the scale grating is in Littrow configuration. So it diffracts back, passing through QW1 and then the centre PBS and incidents into circular polarization configuration 1.

The R-T and T-T beams are both P-polarized. They pass through QW2 whose fast axis is also 45.0° in the coordinate system, same to QW1. Then

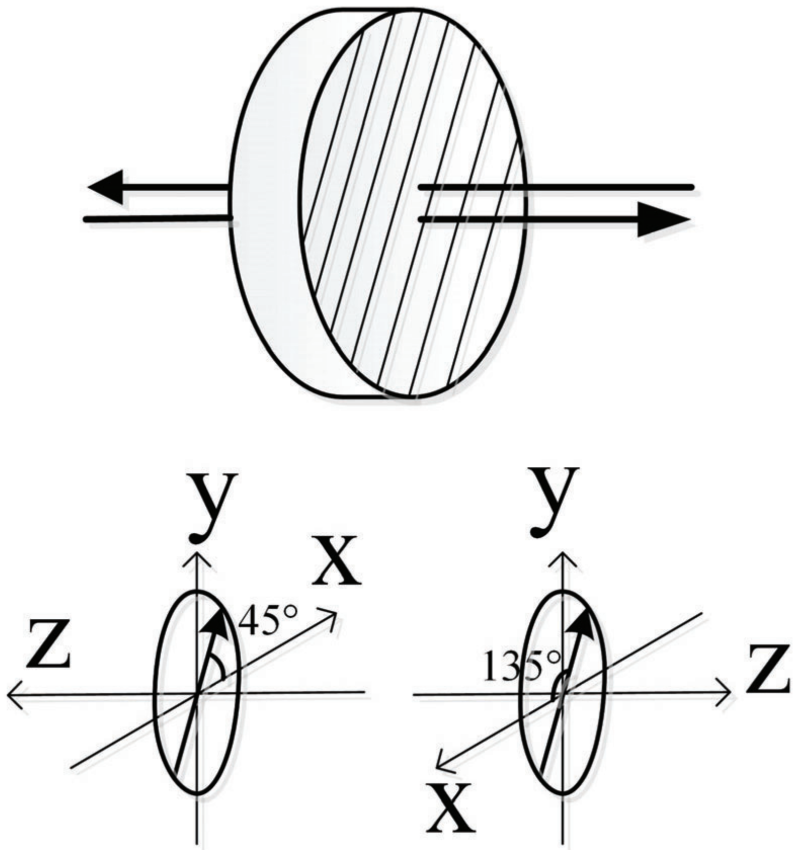

FIGURE 4
Angle of the plates in different directions.

these two laser beams are both reflected by Mirror 4 and turned into a direction where the scale grating is also in Littrow configuration. They diffract back and pass through QW2 again. Then they are reflected by the centre PBS and, respectively, incident into Circular Polarization Configuration 1 and Circular Polarization Configuration 2.

The circular polarization configuration is a classical phase solution structure widely used in homodyne laser interferometer [17]. It is composed of two PBSs, a BS, a half-wave plate, a quarter-wave plate, a compensation plate and four detectors. QW3 is a quarter-wave plate whose fast axis is 45.0° in the coordinate system as shown in Figure 5(a). HW4 is a half-wave plate whose fast axis is 22.5° in the coordinate system as shown in Figure 5(b). CW5 is a compensation plate in order to make the length of the path same. The circular polarization configuration will divide the laser beams incident into four pieces which finally form four interferometer fingers with

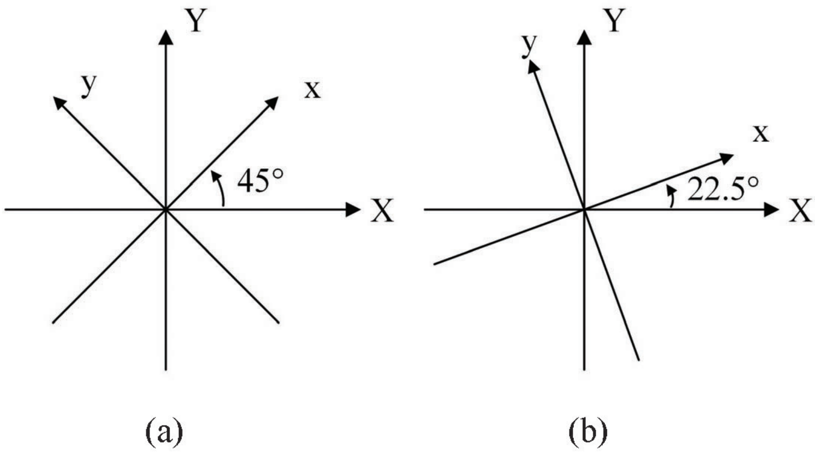

FIGURE 5
Directions of the wave plates for (a) the fast axis of QW3 and (b) the fast axis of HW4.

respectively 90.0° phase difference. Further information will be introduced below. Using two groups of circular polarization configurations, we can get two groups of phase signals which can be used to solve the displacement of the scale gratings.

3 MEASUREMENT PRINCIPLE

The polarization state of the optical structure can be expressed using Jones Matrix. The laser beam is set 45.0° in the coordinate system. Its polarization state can be written as

$$\overrightarrow{e_0} = \frac{\sqrt{2}}{2}\begin{bmatrix}1\\1\end{bmatrix}E_0 e^{i\theta_0} \tag{1}$$

where e is optical vector of laser beam, E is its amplitude and θ is its phase angle. The subscripts represent different laser beams according to their trajectories such as e_0 is the optical vector of the laser generated by the laser source, same as follows.

As we can see, the laser is split into four beams: R-R; R-T; T-R; and T-T after passing through the optical sensor head. Table 1 lists the mathematical expression of Jones Matrix of corresponding optics. Loss of laser power passing through these components as well as diffraction is not taken into consideration as it will not change polarization state; thus the mathematical expression of the grating in Littrow configuration is the same to mirrors.

TABLE 1
Polarization of optics in sensor head.

Polarization of the Optics	Mathematical Expression
Mirror 1, 2, 3 and 4	$\begin{bmatrix} -1 & \\ & 1 \end{bmatrix}$
BS(T)	$\frac{\sqrt{2}}{2}\begin{bmatrix} 1 & \\ & 1 \end{bmatrix}$
BS(R)	$\frac{\sqrt{2}}{2}\begin{bmatrix} -1 & \\ & 1 \end{bmatrix}$
PBS(T)	$\begin{bmatrix} 1 & \\ & 0 \end{bmatrix}$
PBS(R)	$\begin{bmatrix} 0 & \\ & 1 \end{bmatrix}$
QW1(45°), QW2(45°) rotation of fast axis	$\frac{\sqrt{2}}{2}\begin{bmatrix} 1 & -\mathrm{i} \\ -\mathrm{i} & 1 \end{bmatrix}$
QW1(135°), QW2(135°) rotation of fast axis	$\frac{\sqrt{2}}{2}\begin{bmatrix} 1 & \mathrm{i} \\ \mathrm{i} & 1 \end{bmatrix}$
Scale grating	$\begin{bmatrix} -1 & \\ & 1 \end{bmatrix}$

The path of R-R beam in the optical sensor head is: R-R: BS(R)→M1→PBS(R) →QW1(45°) →M3→G(+1)→M3→QW1(135°)→PBS(T). Its polarization can be expressed as

$$\begin{aligned}\overrightarrow{e_{R-R}} &= J_{PBS(T)}J_{QW1(135°)}J_{M3}J_{G(+1)}e^{i\Delta\theta_{+1}}J_{M3}J_{QW1(45°)}J_{PBS(R)}J_{M1}J_{BS(R)}\overrightarrow{e_0} \\ &= \frac{1}{2}\begin{bmatrix} i \\ 0 \end{bmatrix}E_0e^{i(\theta_0+\Delta\theta_{+1})}\end{aligned} \tag{2}$$

where J is the mathematical expression of the Jones Matrix and its subscript represents the corresponding optical component listed in Table 1, and $\Delta\theta$ is the phase change of diffraction beams in a Littrow configuration introduced by grating displacement and its subscript represents different diffraction orders, the same below.

The path of the R-T beam in the optical sensor head is: R-T: BS(R)→M1→PBS(T) →QW2(45°) →M4→G(−1)→M4→QW2(135°)→ PBS(R). Its polarization can be expressed as

$$\begin{aligned}\overrightarrow{e_{R-T}} &= J_{PBS(R)}J_{QW2(135°)}J_{M4}J_{G(-1)}e^{i\Delta\theta_{-1}}J_{M4}J_{QW2(45°)}J_{PBS(T)}J_{M1}J_{BS(R)}\overrightarrow{e_0} \\ &= \frac{1}{2}\begin{bmatrix}0\\-i\end{bmatrix}E_0e^{i(\theta_0+\Delta\theta_{-1})}\end{aligned} \tag{3}$$

The R-R and R-T beams both eventually incident into Circular Polarization Configuration 1. The polarization state of the combined beam is

$$\overrightarrow{e_{R-R}}+\overrightarrow{e_{R-T}}=\frac{1}{2}\begin{bmatrix}e^{i\Delta\theta_{+1}}\\ \text{-}e^{i\Delta\theta_{-1}}\end{bmatrix}E_0e^{i\left(\theta_0+\frac{\pi}{2}\right)} \tag{4}$$

The path of the T-R beam in the optical sensor head is: T-R: BS(T)→PBS(R) →QW1(45°) →M2→QW1(135°)→PBS(T). Its polarization state of the beam can be expressed as

$$\overrightarrow{e_{T-R}}=J_{PBS(T)}J_{QW1(135°)}J_{M2}J_{QW1(45°)}J_{PBS(R)}J_{BS(T)}\overrightarrow{e_0}=\frac{1}{2}\begin{bmatrix}i\\0\end{bmatrix}E_0e^{i\theta_0} \tag{5}$$

The path of the T-T beam in the optical sensor head is: T-T: BS(T)→PBS(T) →QW2(45°) →M4→G(-1)→M4→QW2(135°)→PBS(R). The polarization state of the beam, same to R-T beam, is

$$\begin{aligned}\overrightarrow{e_{T-T}} &= J_{PBS(R)}J_{QW2(135°)}J_{M4}J_{G(-1)}e^{i\Delta\theta_{-1}}J_{M4}J_{QW2(45°)}J_{PBS(T)}J_{BS(T)}\overrightarrow{e_0} \\ &= \frac{1}{2}\begin{bmatrix}0\\-i\end{bmatrix}E_0e^{i(\theta_0+\Delta\theta_{-1})}\end{aligned} \tag{6}$$

The T-R and T-T beams both eventually incident into Circular Polarization Configuration 2 and the polarization state of the combined beams is

$$\overrightarrow{e_{T-R}}+\overrightarrow{e_{T-T}}=\frac{1}{2}\begin{bmatrix}1\\ e^{i\Delta\theta_{-1}}\end{bmatrix}E_0e^{i(\theta_0+\frac{\pi}{2})} \tag{7}$$

As has been mentioned before, the circular polarization configuration is able to adjust the polarization state of the laser beams incident and solve the difference of the phase. The polarization direction of the laser beams are respectively S-polarization and P-polarization. Assume the polarization states of the two incident beams are

$$\begin{cases} \overrightarrow{e_s} = \begin{bmatrix} 1 \\ 0 \end{bmatrix} E_s e^{i\theta_s} \\ \overrightarrow{e_p} = \begin{bmatrix} 0 \\ 1 \end{bmatrix} E_p e^{i\theta_p} \end{cases} \tag{8}$$

where E_s is the amplitude of the optical vector of the S-polarization beam and θ_s is its phase angle. So it is with P-polarization beam. As shown in Figure 6, the beams incident first pass through a quarter-wave plate (QW3) whose fast axis is also set 45° in the coordinate system. The polarization state changes and can be written as

$$\frac{\sqrt{2}}{2}\begin{bmatrix} 1 & -i \\ -i & 1 \end{bmatrix}\begin{bmatrix} E_s e^{i\theta_s} \\ E_p e^{i\theta_p} \end{bmatrix} = \frac{\sqrt{2}}{2}\begin{bmatrix} E_s e^{i\theta_s} \text{-} iE_p e^{i\theta_p} \\ E_p e^{i\theta_p} - iE_s e^{i\theta_s} \end{bmatrix} \tag{9}$$

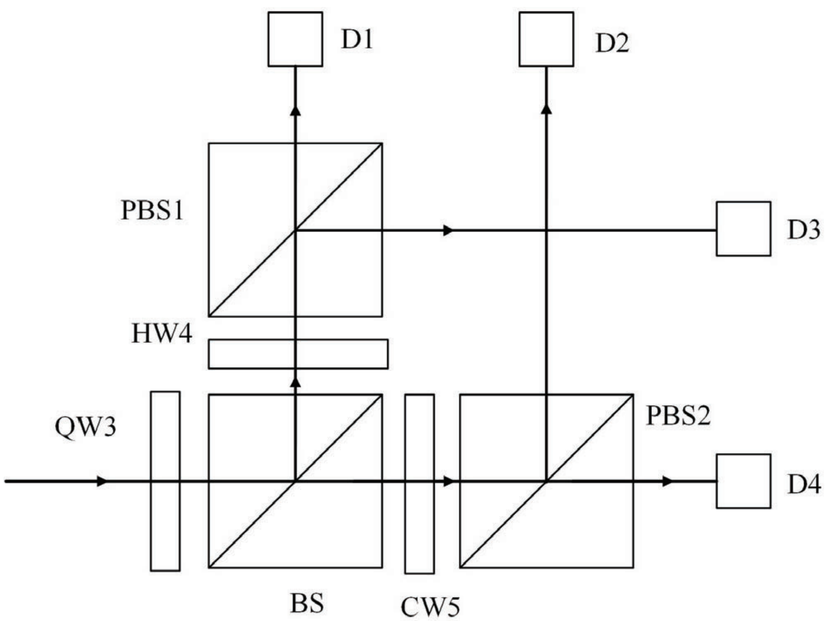

FIGURE 6
Schematic diagram of the circular polarization configuration.

Then, the laser beams pass through a BS and the transmitted amplitude of each laser beam attenuates but the polarization state does not change. Then passing through a recompensed plate and PBS2 the beams are, respectively, received by Detector 2 and Detector 4. The vector mathematical expression of the laser beam is given by

$$\begin{cases} E_2 = \frac{1}{2}\left(E_s e^{i\theta_s} \text{-} iE_p e^{i\theta_p}\right) \\ E_4 = \frac{1}{2}\left(E_p e^{i\theta_p} \text{-} iE_s e^{i\theta_s}\right) \end{cases} \tag{10}$$

The mathematical expression of the power of the laser beam can be obtained from

$$\begin{cases} I_2 \propto \frac{1}{4}\left(E_s^{\ 2} + E_p^{\ 2} + 2E_s E_p \cos\left(\theta_s - \theta_p + \frac{\pi}{2}\right)\right) \\ I_4 \propto \frac{1}{4}\left(E_s^{\ 2} + E_p^{\ 2} + 2E_s E_p \cos\left(\theta_s - \theta_p + \frac{3\pi}{2}\right)\right) \end{cases} \tag{11}$$

where I is the power of the laser spot detected by corresponding detector.

The reflected beams of the BS pass through HW4 whose fast axis is set 22.5° in the coordinate system. The polarization state changes into

$$\frac{\sqrt{2}}{2}\begin{bmatrix} 1 & 1 \\ 1 & -1 \end{bmatrix}\frac{1}{2}\begin{bmatrix} E_s e^{i\theta_s} \text{-} iE_p e^{i\theta_p} \\ E_p e^{i\theta_p} - iE_s e^{i\theta_s} \end{bmatrix} = \frac{1}{2}\begin{bmatrix} E_s e^{i\left(\theta_s + \frac{3}{4}\pi\right)} + E_p e^{i\left(\theta_p + \frac{3}{4}\pi\right)} \\ E_s e^{i\left(\theta_s \text{-} \frac{1}{4}\pi\right)} + E_p e^{i\left(\theta_p + \frac{3}{4}\pi\right)} \end{bmatrix} \tag{12}$$

The mathematical expression of the lasers power can be given by

$$\begin{cases} I_1 \propto \frac{1}{4}\left(E_s^{\ 2} + E_p^{\ 2} + 2E_s E_p \cos\left(\theta_s - \theta_p\right)\right) \\ I_3 \propto \frac{1}{4}\left(E_s^{\ 2} + E_p^{\ 2} + 2E_s E_p \cos\left(\theta_s - \theta_p + \pi\right)\right) \end{cases} \tag{13}$$

By simple operation we can eliminate the interference of signal amplitude and DC noise and solve the phase difference of the incident beams:

$$\theta_s - \theta_p = \tan^{-1}\left(\frac{I_2 - I_4}{I_1 - I_3}\right) \tag{14}$$

In the two degrees of freedom linear encoder, the polarization state of the incident beams are, respectively, shown in Equation (4) and Equation (7). Using two circular polarization configurations, we can solve the Doppler phase change of the scale grating:

$$\begin{cases} \alpha_1 = \Delta\theta_1 - \Delta\theta_{-1} \\ \alpha_2 = \Delta\theta_{-1} \end{cases} \tag{15}$$

where $\alpha 1$ and $\alpha 2$ are the phase calculation results of Circular Polarization Configuration 1 and Circular Polarization Configuration 2, respectively. The Doppler phase caused by scale grating's motion is different in different directions. We set *X*-direction as the grating vector direction and the *Z*-direction as the grating normal direction. The Doppler phase caused by the motion of the scale grating along the *X*-direction is

$$\begin{cases} \Delta\theta_{-1} = 2\pi \dfrac{s_x}{d} \\ \Delta\theta_{+1} = -2\pi \dfrac{s_x}{d} \end{cases} \tag{16}$$

where *d* is the pitch of the grating and sx is its displacement along *X*-direction. While the Doppler phase caused by the motion of the scale grating along the *Z*-direction is

$$\Delta\theta_{-1} = \Delta\theta_{+1} = 2\pi \frac{s_z(1+\cos\gamma)}{\lambda} \tag{17}$$

where γ is the diffraction angle and s_z is the displacement of the grating along the *Z*-direction. By detecting the phase differences output by circular polarization configurations we can solve the displacement of the scale grating:

$$\begin{cases} s_x = \dfrac{\alpha_1}{4\pi} d \\ s_z = \dfrac{\alpha_2}{2\pi\left(1+\cos\gamma\right)} d \end{cases} \tag{18}$$

In a word, the laser linear encoder is able to measure two degrees of freedom. Given the Littrow configuration, the encoder can always work as long as the laser spots are on the scale gratings and its measuring area is discussed below.

4 THE MEASURING AREA OF THE LINEAR ENCODER AND ITS ALIGNMENT TOLERANCE

The linear encoder is able to measure two degrees of freedom motion and its measuring area is affected by the parameters of the system. As the optical sensor is designed in Littrow configuration, the translation of the scale grating will not change the diffraction beams' direction and position. So the linear encoder is always able to work as long as the laser spots are on the scale gratings.

As has mentioned before, three diffraction beams are respectively reflected to the scale grating which is in Littrow configuration. Two of them (R-R and T-T) are minus one diffracted order while the other one (R-T) is plus one diffracted order. We create a XY Cartesian coordinate at the intersection point of R-T and T-T beam as shown in Figure 7. The x-axis and the grating vector are in same direction and the y-axis and the grating normal direction are in same direction. In Figure 7, γ is the diffraction angle, D is the distance between R-R and T-T beams along the y-axis and L is the length of the gratings in this direction. The laser beams in the coordinate system can be expressed by the functions

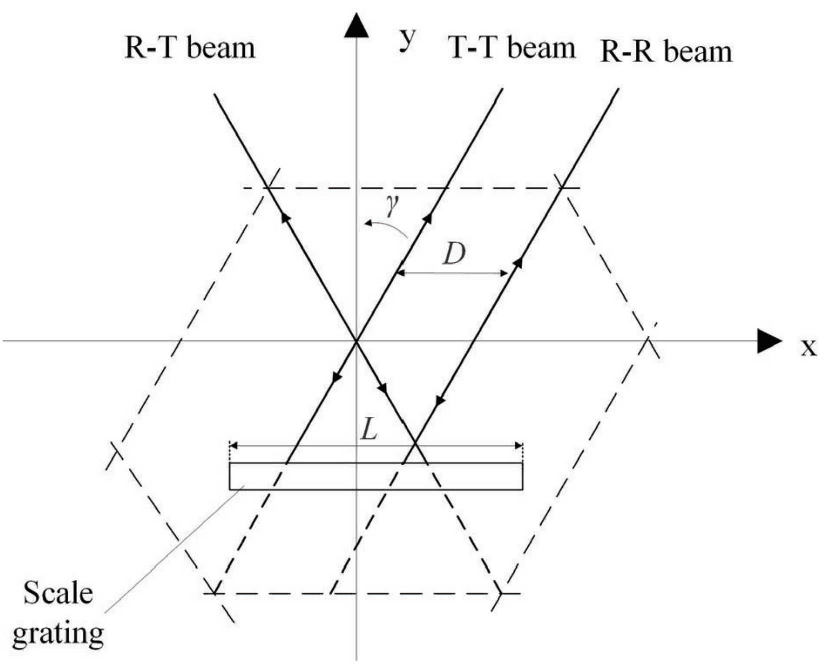

FIGURE 7
Analysis of the measuring area.

$$\begin{cases} y = x\cot\gamma \\ y = (x-D)\cot\gamma \\ y = -x\cot\gamma \end{cases} \tag{19}$$

Assume the edge point on the left side of the scale gratings in the coordinate system is (x0, y0). The diffraction beams' spots are all on the gratings when the following inequalities are established:

$$\begin{cases} x_0 \le \dfrac{y_0}{\cot\gamma} \le x_0 + l \\ x_0 \le \dfrac{y_0}{\cot\gamma} + D \le x_0 + l \\ x_0 \le -\dfrac{y_0}{\cot\gamma} \le x_0 + l \end{cases} \tag{20}$$

These inequalities become a closed area that is the motion range of the left edge point on the scale grating. By considering the length of the grating, we get the actual measuring area surrounded by dotted lines shown in Figure 7. One can see the area is a parallel hexagon. Its horizontal width is affected by *L* and *D*. By employing longer gratings and reducing the distance of the parallel beams we can get wider measuring area. Its vertical width along the *y*-axis can be written as

$$\Delta y = \left(L - \frac{D}{2}\right)\cot\gamma \tag{21}$$

where Δy is the width which is also the maximum *z*-axis displacement of the grating. Besides employing longer gratings and reducing the distance of the parallel beams, we can also choose proper wave length and grating pitch to make the diffraction angel γ smaller in order to get larger measuring area. The angle relationship is cotangent. So the measuring range along *y*-axis can be extended to a larger size.

As to the alignment tolerance, it only needs to consider the rotation of the grating including roll, pitch and yaw. Optical ray tracing in optical software was adopted to study the alignment tolerance of the linear encoder and its simulation model is shown in Figure 8. The model was simplified without quarter-wave plates and circular polarization configurations which have little influence on it. Schematic diagram of position of misaligned beam spots under different run out conditions yielded by the optical ray tracing are shown in Figure 9. The separation by all the photodiodes between the two beams

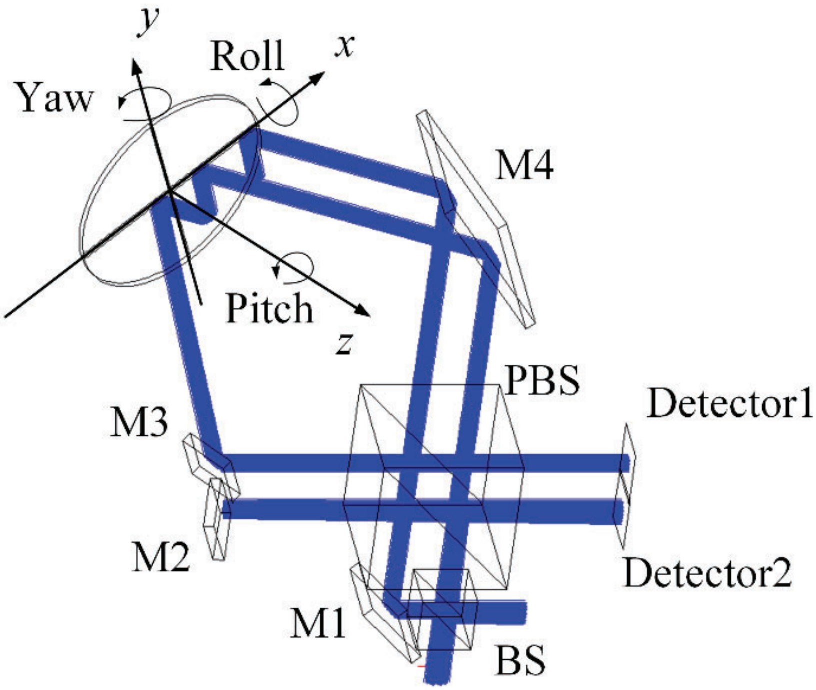

FIGURE 8
Simulation model of the laser linear encoder configuration.

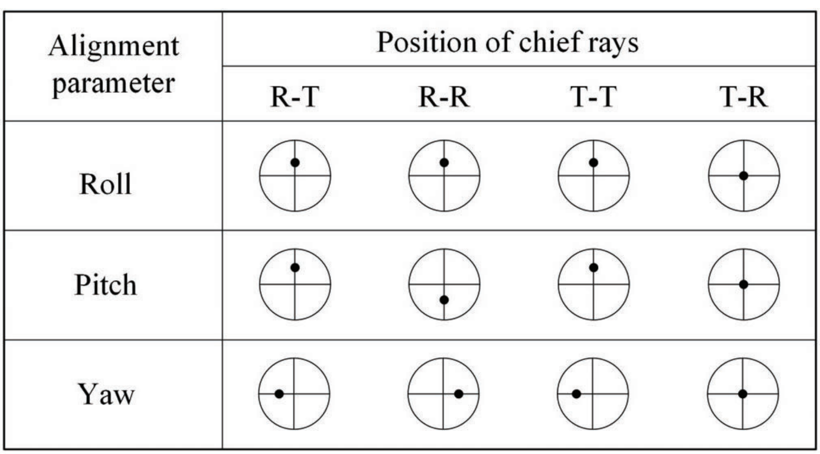

FIGURE 9
Positions of the misaligned laser beam spots under different run out conditions.

captured should be less than one fourth of the diameter of the beam which is 0.9 mm in the actual setup. As we can see, the position of T-R beam is not influenced by different run out conditions .The T-R and T-T beam is always separated under different run out conditions. Roll was found to cause R-T and R-R beam to move together and the alignment tolerance turned out to be 3.71 arc min. Pitch and yaw were found to cause R-T beam and R-R beam to separate from each other and the alignment tolerance were 3.10 arc min and 1.42 arc min, respectively. As we can see, the alignment tolerance of laser linear encoder can at least meet the application needs.

5 EXPERIMENTAL CONFIGURATION AND SYSTEM PERFORMANCE

Performance of a commercial fibre interferometer (FPS3010; Attocube, Inc.) was compared with the laser linear encoder to evaluate the measurement accuracy of the latter. Figure 10 shows the experimental structure for verification and Figure 11 is a photograph of the experimental configuration which we used to install optical components of the linear encoder including PBSs (PBS0110/PBS0125; Union Optic, Inc.), BS (BS012; Thorlabs, Inc.), mirrors (LLM0012–45/ LLM0025–45; Union Optic, Inc.), QWs (WPZ4320; Union

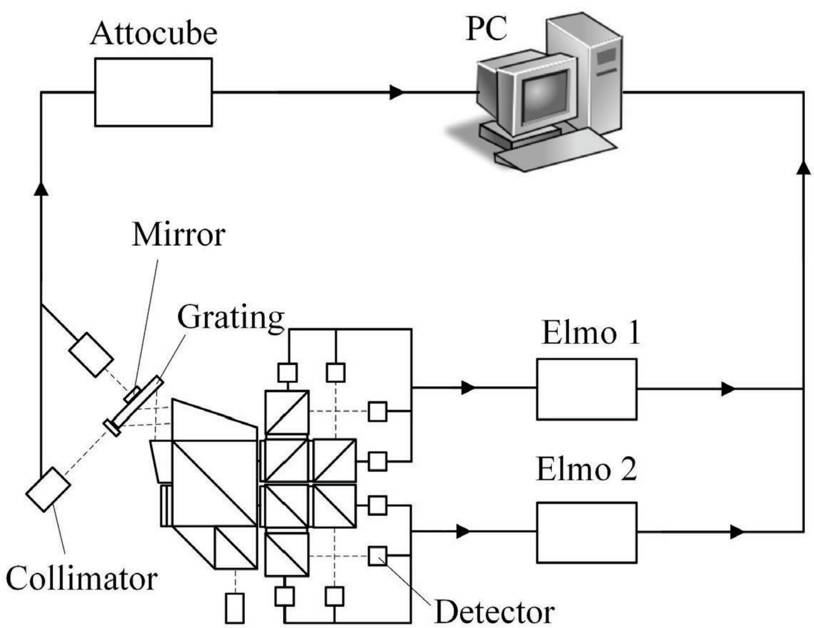

FIGURE 10
Schematic diagram of the experimental configuration for verification of the laser linear encoder.

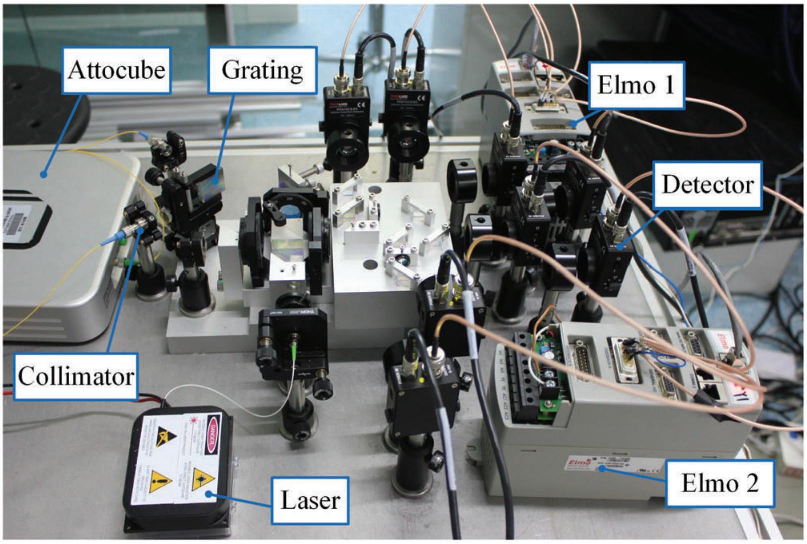

FIGURE 11
Photograph of the experimental configuration of the laser linear encoder.

Optic, Inc.) and HWs (WPZ2310; Union Optic, Inc.). Compensation plates were not necessary and were not employed. The experimental configuration is specially designed and machined and its machining accuracy was measured by three-coordinate measuring machine which was proved to meet the design requirements. The wave length of the laser is 1.55 μm which is constructed by a laser source (1550FSZ; Sichuan Tengguang; Inc.). The diameter of the laser beam is approximately 0.9 mm. We employed a commercial grating (GR25–0616; Thorlabs, Inc.) as the scale grating whose pitch is approximately 1.660 μm. The scale grating was mounted on an adjustable mount (KM100C; Thorlabs, Inc.) which is on a table stacked by two one degree of freedom manual displacement tables (MS1S/M; Thorlabs, Inc.) whose largest range of displacement is about 6.0 mm. The adjustable mount which can yaw and roll is used to align the grating with the linear encoder. As the grating should be set in Littrow configuration, the diffraction beams should be adjusted coincident with the incident beams. The laser is 1.55 μm and is invisible. We employed a laser viewing card (VRC2; Thorlabs, Inc.) to help adjust the grating.

The detectors (PDA10CS-EC; Thorlabs, Inc.) conversed the interferometer fingers into analogue signals and the signals were respectively introduced into two analogue drivers (Cor-7/230; Elmo, Inc.) whose subdivision multiple was set 4096. Thus the readout solution of the linear encoder was 0.407 nm in the X-direction and 0.214 nm in the Z-direction. The results were directly introduced into two computers to be recorded. As shown in

Figure 10, we stack a mirror on the back of the scale grating and another one on the side face of it. As the collimators of the fibre interferometer have to be aligned to the mirrors, the displacement range was limited to $2 \times 2\,\text{mm}^2$.

We measured a stepping motion along the X- and Y-direction for 2.0 mm. In the X-direction, the maximum positioning error is 4.270 μm with a standard deviation of 1.250 μm and in the Z-direction it is 2.660 μm with a standard deviation of 0.691 μm. It can be seen that the measurement errors were dominated by the cosine error which is caused by inevitable misalignment between the measuring directions of the fibre interferometer and the linear encoder. Figure 12 shows the residual errors after least-squares line fitting in the X- and Z-direction. As we can see, the maximum positioning error turned out to be 0.261 μm with a standard deviation of 0.134 μm in the X-direction and 0.211 μm with a standard deviation of 0.070 μm in the Z-direction. The experiment was conducted under non-environmentally controlled conditions. Figure 13 shows the experiment results of noise level measurements in the laboratory. The noise level of the proposed system for linear displacement is about 51.700 nm (3× standard deviation) in X-direction and 65.200 nm in the Z-direction. For the two degrees of freedom measuring test, the movement tables were respectively moved in its max range and the interference signals were not lost when the grating was moving in two degrees of freedom.

The measurement environment, in fact, is quite unstable and the readout solution of the linear encoder is totally submerged in the environmental noise. Figure 14 shows the ambient noise level measured by fibre interferometer in the X-direction. Figure 14(a) is measurement time-domain diagram and Figure 14(b) is measurement frequency domain diagram. As we can see, the vibration amplitude of the result is close to 50.000 nm which is consistent with the result of laser linear encoder. Its energy is mainly concentrated in low frequency which indicates that ambient vibration and temperature changes may introduce most of the measurement error. The experiment should be controlled and structure of the measuring device should be made more robust and compact to get better performance. Low-pass filters should also be used to filter circuit noise. In a word, the measuring principle of the two degrees of freedom linear encoder has been verified and its performance can be improved by several methods.

6 CONCLUSIONS

We proposed a new optical sensor head designed in Littrow configuration for laser linear encoder which can directly measure X- and Z-direction displacement of a linear stage using one-dimensional (1-D) gratings. The measuring range along the Z-direction is extremely enlarged compared with traditional encoders. The optical configuration was successfully constructed and the measurement performance was evaluated and analysed. The system

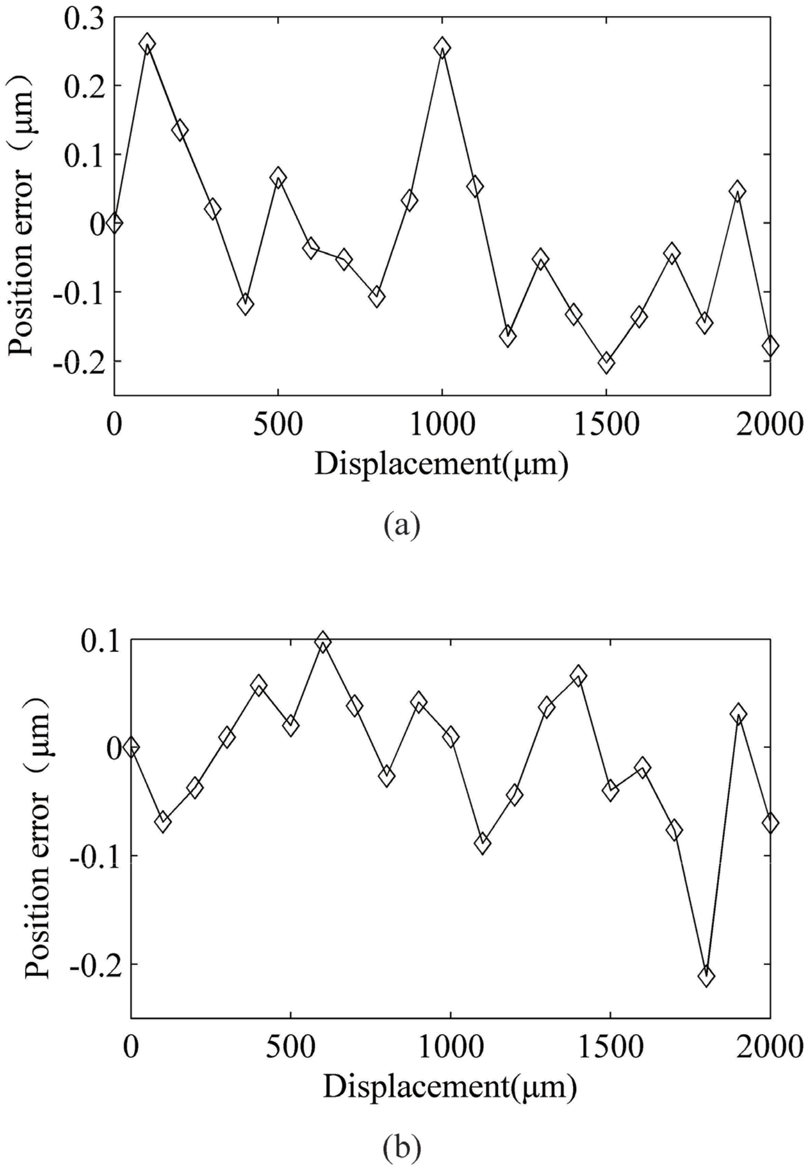

FIGURE 12
Graphs showing the position error between encoder and interferometer in (a) the *X*-direction and (b) the *Z*-direction.

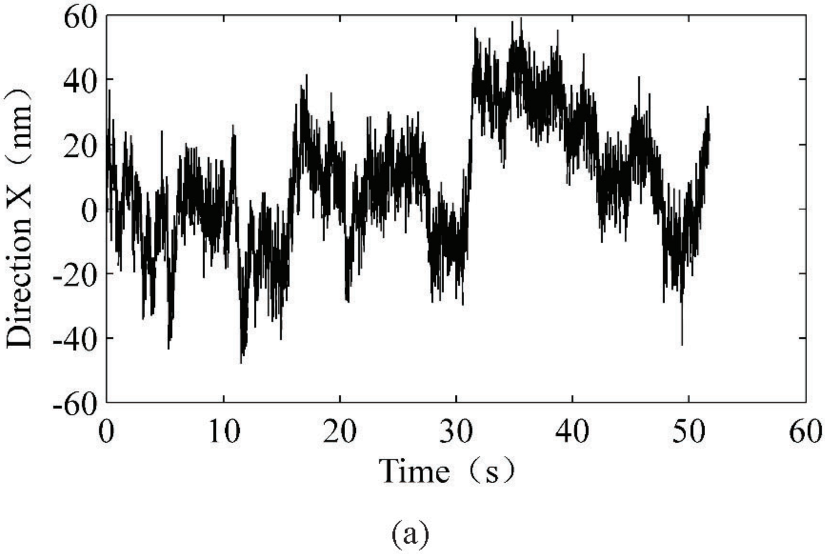

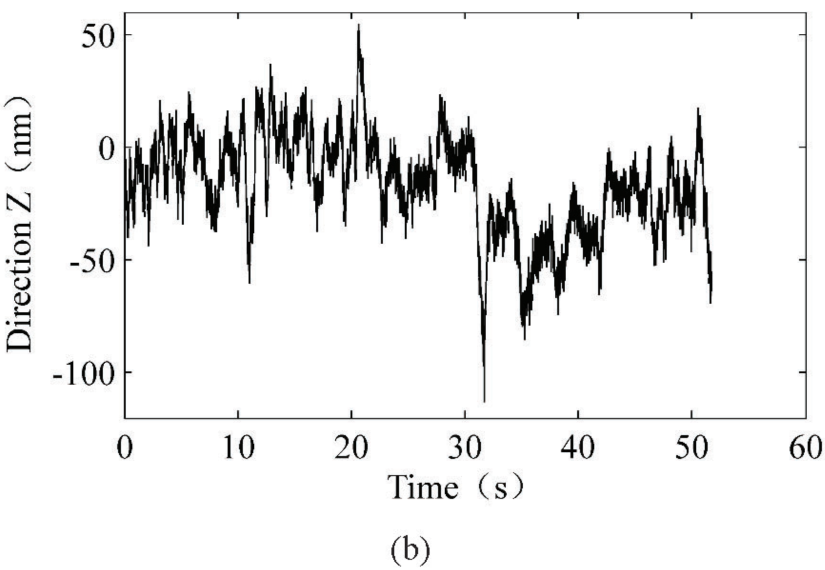

FIGURE 13
Graphs showing the noise level measurements of the laser linear encoder in (a) the *X*-direction and (b) the *Z*-direction.

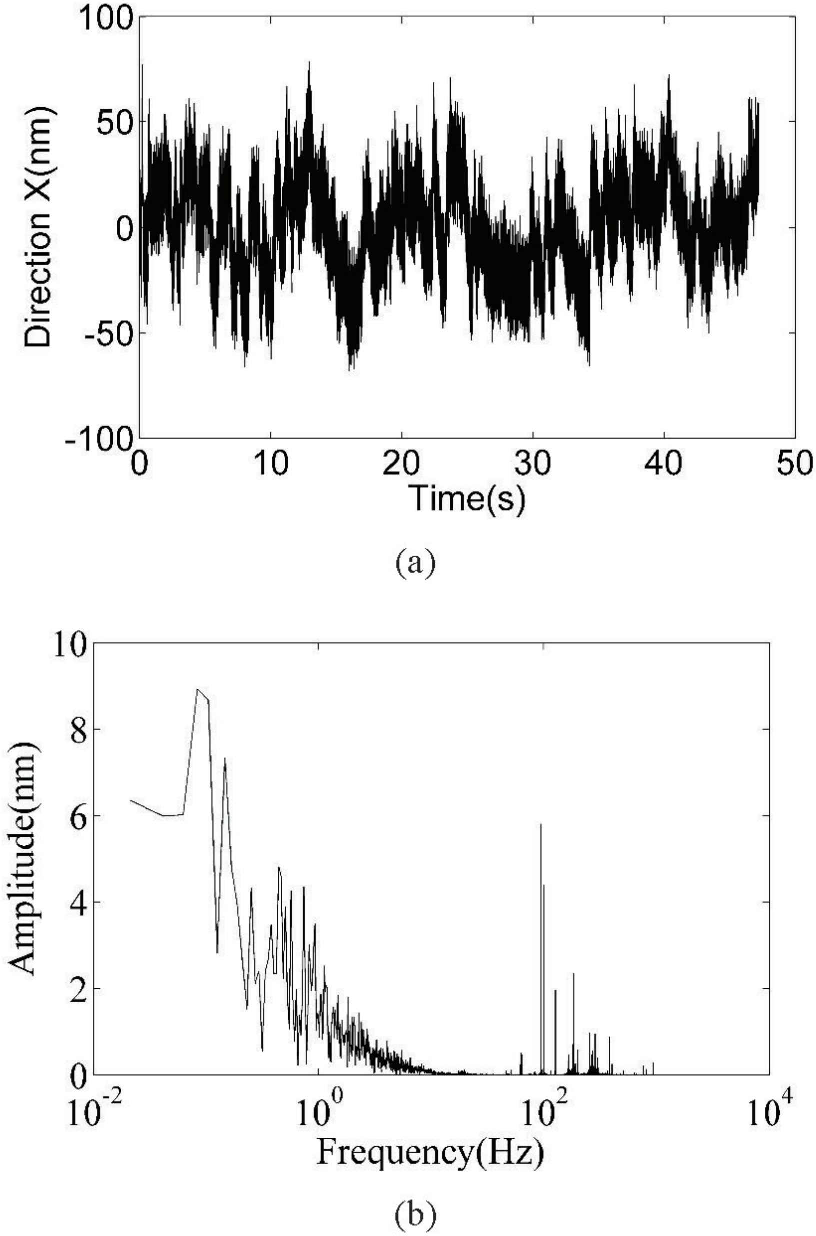

FIGURE 14
Graphs of the ambient noise level measured by the fibre interferometer in the *X*-direction for (a) the measurement time domain and (b) the measurement frequency domain.

has resolutions of 51.700 nm in the *X*-direction and 65.200 nm in the *Z*-direction. It was confirmed that the linear encoder is able to measuring large scale motion in two degrees of freedom. Further study on environment disturbance and mechanical structure will be done in order to get better measurement performance.

NOMENCLATURE

d	Pitch of the grating (m)
D	Distance between R-R and T-T laser beams along the y-axis (m)
e	Optical vector of the laser beam
E	Amplitude of the optical vector
I	Power of the laser (W)
J	Mathematical expression of the Jones Matrix
L	Length of the grating (m)
s	Displacement of the grating (m)

Greek symbols

γ	Diffraction angle (°)
θ	Phase angle of the optical vector(°)

REFERENCES

[1] Bobroff, N. Recent advances in displacement measuring interferometry. *Measurement Science & Technology* **4**(9) (1998), 907–926.

[2] Fan K.C., Lee B.C. and Chung Y.C. A planar laser diffraction encoder in Littrow configuration for 2D nanometric positioning. *International Journal of Automation & Smart Technology* **2** (2011), 93–99.

[3] Wu C.C., Wu W.J., Pan Z.S. and Lee C.K. Laser linear encoder with both high fabrication and head-to-scale tolerances. *Applied Optics* **46**(16) (2007), 3169–3176.

[4] Kao C.F., Lu S.H., Shen H.M. and Fan K.C. Diffractive laser encoder with a grating in Littrow configuration. *Japanese Journal of Applied Physics* **47**(3) (2008), 1833–1837.

[5] Zhao B., Wang L., Xu M.E., Zhao H. and Liu X.D. A displacement measuring system based on grating double diffraction. *Proceedings of SPIE* **9446** (2015), 94464J-7.

[6] Wang P., Zhang Z. and Yan P. A low cost measurement method for a large stroke XY nano-positioner by using linear optical encoders. *34th Chinese Control Conference (CCC)*. 28–30 July 2015, Hangzhou, China. pp. 8325–8330.

[7] Kimura A., Wei G., Arai Y. and Zeng L. Design and construction of a two degrees of freedom linear encoder for nanometric measurement of stage position and straightness. *Precision Engineering* **34**(1) (2010), 145–155.

[8] Liu C.H. and Cheng C.H. Development of a grating based multi-degree-of-freedom laser linear encoder using diffracted light. *Sensors & Actuators A: Physical* **181**(7) (2012), 87–93.

[9] Huang H.L., Liu C.H., Jywe W.Y., Wang M.S. and Fang T.H. Development of a three-degree-of-freedom laser linear encoder for error measurement of a high precision stage. *Review of Scientific Instruments* **78**(6) (2007), 066103–3.

[10] Akihide K., Gao W. and Zeng L. Position and out-of-straightness measurement of a precision linear air-bearing stage by using a two degrees of freedom linear encoder. *Measurement Science & Technology* **21**(5) (2010), 54005–54014.

[11] Chen C.K., Liu C.H. and Cheng C.H. Multi-DOF incremental optical encoder with laser wavelength compensation. *Smart Science* **1**(1) (2013), 44–52.

[12] Hsieh H.L. and Pan S.W. Development of a grating-based interferometer for six-degree-of-freedom displacement and angle measurements. **23**(3) (2015), 2451–2465.

[13] Liu Y., Yuan M., Cao J., Cui J. and Tan J. Use of two planar gratings to measure 3-DOF displacements of planar moving stage. *IEEE Transactions on Instrumentation & Measurement* **64**(1) (2015), 163–169.

[14] Fan K.C., Liao B.H., Chung Y.C. and Chung T.T. Displacement measurement of planar stage by diffraction planar encoder in nanometre resolution. *2012 IEEE International Instrumentation and Measurement Technology Conference (I2MTC)*. 13–16 May 2012, Graz, Austria. pp. 894–897.

[15] Hsieh H.L., Chen J.C., Lerondel G. and Lee J.Y. Two-dimensional displacement measurement by quasi-common-optical-path heterodyne grating interferometer. *Optics Express* **19**(19) (2011), 9770–9782.

[16] Jie L., Guan J. and Jin P. Grating encoder for wide range three-axis displacement measurement. *Proceedings of SPIE* **9446** (2015), 944602–8.

[17] Eom T.B., Kim J.Y. and Jeong K. The dynamic compensation of nonlinearity in a homodyne laser interferometer. *Measurement Science & Technology* **12**(10) (2001), 1734–1738.